

Autonomous out-of-equilibrium Maxwell's demon for controlling the energy fluxes produced by thermal fluctuations

Sergio Ciliberto*

Université Lyon, Ens de Lyon, Université Claude Bernard, CNRS, Laboratoire de Physique, UMR 5672, F-69342 Lyon, France



(Received 13 September 2020; accepted 10 November 2020; published 25 November 2020)

An autonomous out-of-equilibrium Maxwell's demon is used to reverse the natural direction of the heat flux between two electric circuits kept at different temperatures and coupled by the electric thermal noise. The demon does not process any information, but it achieves its goal by using a frequency-dependent coupling with the two reservoirs of the system. There is no mean energy flux between the demon and the system, but the total entropy production (system + demon) is positive. The demon can be power supplied by thermocouples. The system and the demon are ruled by equations similar to those of two coupled Brownian particles and of the Brownian gyrator. Thus our results pave the way to the application of autonomous out-of-equilibrium Maxwell's demons to coupled nanosystems at different temperatures.

DOI: [10.1103/PhysRevE.102.050103](https://doi.org/10.1103/PhysRevE.102.050103)

Nowadays the notion of Maxwell's demon (MD) is generically used to indicate mechanisms that allow a system to execute tasks in apparent violation of the second law of thermodynamics, such as, for example, to produce work from a single heat bath and to transfer heat from cold to hot sources. To obtain this result the demon does not exchange energy with the system but it has a positive entropy production rate, which compensates the negative entropy production of the system. In general the increase in entropy is induced by the fact that the demon needs to analyze the information that it gathers on the system status [1,2]. In experiments this apparent violation of the second law is obtained by feedback mechanisms which often require the use of external devices such as analog-to-digital (A/D) converters, computers, etc. [3–6]. Several smart experiments [7–9] have implemented this feedback locally, constructing in this way autonomous Maxwell's demons, which do not need the use of external devices as the measure and the feedback are performed in the same place. Several autonomous Maxwell's demons have been theoretically developed [10–14], but they can be of difficult practical implementation in several devices such as colloidal particles and mesoscopic electric circuits at room temperature. However, Refs. [15,16] introduced a new paradigm of MD based on an out-of-equilibrium device, which does not elaborate any information about the system status. It has been shown that the parameters of this device can be suitably tuned in such a way that it does not exchange energy (heat or work) with the system but it has a positive entropy production rate. Thus it has the two main requirements of an autonomous MD and it can be more easily experimentally realized because, in contrast to the commonly used definition of MD, it works without acquiring and analyzing any information about the system status.

We discuss here how to implement an out-of-equilibrium MD (OEMD) [15,16] in electric circuits, which are versatile dynamical systems ruled by coupled Langevin equations [17,18].

Thus our study is quite general because it opens the way to the application of OEMDs to coupled nanosystems modeled by Langevin equations. As an example we will show in this Rapid Communication how an OEMD can be used to reverse the natural direction of the heat flux between two electric circuits kept at different temperatures and coupled by the electric thermal noise [19,20]. In Fig. 1 we sketch the system (gray box) and the demon (yellow box). We chose for the system this specific circuit because the statistical properties of the heat flux have been characterized both theoretically and experimentally [19,20]. Furthermore, it is ruled by the same equations of the Brownian gyrator [21,22] and of two Brownian particles coupled by a harmonic potential and kept at different temperatures [19], making the result rather general.

The system (gray box in Fig. 1) is constituted of two resistances R_1 and R_2 , which are kept at two different temperatures T_1 and $T_2 \geq T_1$. In the figure, the two resistances have been drawn with their associated thermal noise generators η_1 and η_2 , whose power spectral densities are given by the Nyquist formula $|\tilde{\eta}_m|^2 = 4k_B R_m T_m$, with $m = 1, 2$. The coupling capacitance C controls the electrical power exchanged between the resistances and as a consequence the energy exchanged between the two baths. No other coupling exists between the two resistances. The two capacitors C_1 and C_2 represent the sum of the circuit and cable capacitances. All the relevant energy exchanges in the system can be derived by the simultaneous measurements of the voltage V_m ($m = 1, 2$) across the resistance R_m and the currents i_m flowing through them. When $T_1 = T_2$ the system is in equilibrium and exhibits no net energy flux between the two reservoirs. The circuit equations can be written in terms of charges q_m flowing through the resistances R_m , so the measured instantaneous currents are

*sergio.ciliberto@ens-lyon.fr

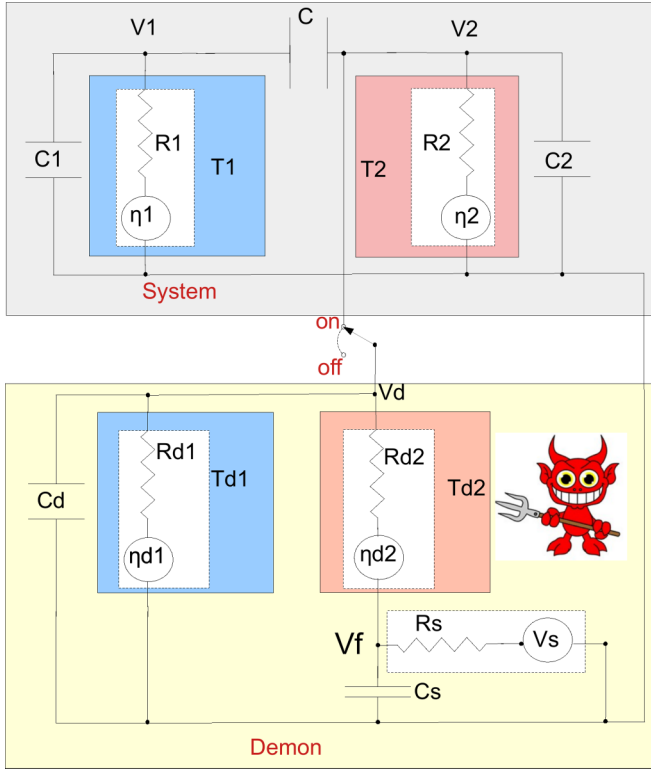


FIG. 1. Diagram of the system (gray box) and of the demon (yellow box). The system is constituted by the two resistances R_1 and R_2 kept respectively at temperature T_1 and T_2 , with $T_2 \geq T_1$. They are coupled via the capacitor C . The capacitors C_1 and C_2 schematize the capacitances of the cables and of the amplifier inputs. The demon (yellow box) is composed of two resistances (R_{d1} and R_{d2}) kept at two different temperatures T_{d1} and T_{d2} . Furthermore, the resistance R_{d2} is driven by a voltage generator V_s whose output is filtered by the low-pass filter composed of the resistance R_s and the capacitance C_s . The four voltage generators η_k ($k = 1, 2, d1, d2$) represent the Nyquist noise voltages of the resistances at the temperatures of the heat baths.

$i_m = \dot{q}_m$. We make the choice of working with charges because the analogy with a Brownian particle is straightforward as q_m is equivalent to the displacement of the particle m [18–20]. A circuit analysis shows that the equations for the charges are

$$R_1 \dot{q}_1 = V_1 - \eta_1, \quad \text{and} \quad R_2 \dot{q}_2 = \eta_2 - V_2, \quad (1)$$

with

$$V_1 = \frac{-q_1(C + C_2) + q_2 C}{X}, \quad (2)$$

$$V_2 = \frac{-q_1 C + q_2(C + C_1)}{X}, \quad (3)$$

where $X = C_2 C_1 + C(C_1 + C_2)$ and η_m is the Nyquist white noise: $\langle \eta_i(t) \eta_j(t') \rangle = 2\delta_{ij} k_B T_i R_j \delta(t - t')$. In Ref. [20] we have shown that Eqs. (1) fully characterize all the thermodynamics properties of the system.

In this system the work and the heat are defined as

$$\dot{W}_m = \frac{C}{X} q_{m'} \dot{q}_m, \quad (4)$$

$$\dot{Q}_m = V_m i_m = V_m \frac{V_m - \eta_m}{R_m}. \quad (5)$$

The quantities \dot{W}_m are identified as the thermodynamic work performed by the circuit m' on $m \neq m'$ and \dot{Q}_m the heat dissipated by the resistance m [17–20,23]. As all the variables are fluctuating, the derived quantities \dot{Q}_m and \dot{W}_m fluctuate too. In Ref. [19] we computed and measured the mean heat flux between the two heat baths, which is given by

$$\langle \dot{Q}_1 \rangle = -\langle \dot{Q}_2 \rangle = \frac{C^2 k_B (T_2 - T_1)}{XY}, \quad (6)$$

where $\langle \cdot \rangle$ stands for mean value and we have introduced the quantity $Y = [(C_1 + C)R_1 + (C_2 + C)R_2]$. We use the convention that the heat extracted from a system reservoir is negative and the heat dissipated is positive.

The out-of-equilibrium demon is sketched in the yellow box in Fig. 1 and it is composed of two resistances (R_{d1} and R_{d2}) kept at two different temperatures T_{d1} and T_{d2} [24]. The two voltage generators η_{d1} and η_{d2} represent the Nyquist noise voltages associated with the two resistances at the heat bath temperatures. Furthermore, the resistance R_{d2} is driven by a voltage generator V_s whose output is filtered by the low-pass filter composed of the resistance R_s and the capacitance C_s . We notice that demon scheme is similar to that of the system, with a coupling capacitance $C \rightarrow \infty$, on which the driving V_s has been added. To design it, we followed the main prescriptions of Ref. [15]: (1) It is out of equilibrium; (2) either T_{d1} or T_{d2} has to be smaller than T_1 ; (3) it produces colored noise, obtained in our case by the source V_s filtered by R_s and C_s ; and (4) it is coupled with the two parts of the system on different frequency ranges, specifically, high frequencies with subsystem 1 and DC coupled with subsystem 2.

The choice of V_s is very important in order to simplify the experimental configuration. Indeed, V_s can be either the thermal fluctuations of R_s with a suitable cutoff imposed by the $R_s C_s$ or an external driving. Many choices are possible and the simplest one is to use $V_s = V_f = \text{const}$ and $R_s = 0$. In such a way V_f is coupled with R_2 only and the thermal noises η_{d1} and η_{d2} are directly coupled with R_2 and high-pass filtered for R_1 . The demon is always out of equilibrium, because, when it is disconnected from the system, the power supplied by V_f is entirely dissipated in the demon resistances producing a mean heat flux towards the demon heat baths, even in the case $T_{d1} = T_{d2}$. This is a simplified version of the original OEMD of Ref. [15] because it requires the use of only one cold source at T_d and a DC signal that can be easily generated by thermocouples making the demon fully autonomous. We will demonstrate that this demon can reverse the heat flux of the system in a wide range of parameters with a zero energy flux (heat and work) with the system.

The connection of the demon to the system changes the current distributions and the energy exchanges. The circuit analysis shows [24] that the currents \dot{q}_k ($k = 1, 2, d1, d2$)

flowing in the resistances R_k are now ruled by the following equations,

$$R_1 \dot{q}_1 = V_1 - \eta_1, \quad (7)$$

$$R_2 \dot{q}_2 = \eta_2 - V_2, \quad (8)$$

$$R_{d1} \dot{q}_{d1} = \eta_{d1} - V_2, \quad (9)$$

$$R_{d2} \dot{q}_{d2} = \eta_{d2} + V_f - V_2, \quad (10)$$

$$V_1 = \frac{-(C_t + C)q_1 + C q_t}{X_t} \quad (11)$$

$$V_2 = \frac{(C_1 + C)q_t - C q_1}{X_t}, \quad (12)$$

where $q_t = (q_2 + q_{d2} + q_{d1})$, $C_t = C_2 + C_d$, and $X_t = C_1 C_t + C(C_1 + C_t)$.

In order to reduce the number of parameters we consider the case $T_d = T_{d1} = T_{d2}$ and $R_{d1} = R_{d2}$. The heat fluxes in the four reservoirs can be computed using $\dot{Q}_k = v_k \dot{q}_k$, where v_k is the potential difference on the resistance R_k [24]. Introducing the following parameters, $R_d = R_{d1} R_{d2} / (R_{d1} + R_{d2})$, $R_t = R_d R_2 / (R_d + R_2)$, $Y_t = R_1(C + C_1) + R_t(C + C_t)$, $A = C^2 k_B / (X_t Y_t)$, $\langle V_2 \rangle = V_t = V_f R_t / R_{d2}$, $B = A R_t [X_t R_t + R_1(C_1 + C)^2] / (R_d R_2 C^2)$, we obtain

$$\langle \dot{Q}_1 \rangle = A \left(\frac{R_t}{R_2} (T_2 - T_1) + \frac{R_t}{R_d} (T_d - T_1) \right), \quad (13)$$

$$\langle \dot{Q}_2 \rangle = -A \frac{R_t}{R_2} (T_2 - T_1) - B(T_2 - T_d) + \frac{V_t^2}{R_2}, \quad (14)$$

$$\begin{aligned} \langle \dot{Q}_d \rangle &= -A \frac{R_t}{R_d} (T_d - T_1) - B(T_d - T_2) \\ &+ \frac{V_f^2 R_t}{R_{d2}} \left(\frac{1}{R_{d1}} + \frac{1}{R_2} \right) - \frac{V_t^2}{R_2}, \end{aligned} \quad (15)$$

$$\langle \dot{W}_f \rangle = \frac{V_f^2 R_t}{R_{d2}} \left(\frac{1}{R_{d1}} + \frac{1}{R_2} \right), \quad (16)$$

where $\langle \dot{Q}_d \rangle = \langle \dot{Q}_{d1} \rangle + \langle \dot{Q}_{d2} \rangle$ is the total heat flux in the demon reservoirs and $\langle \dot{W}_f \rangle$ is the total power supplied by the external generator V_f . The total energy balance demon + system is

$$\langle \dot{Q}_d \rangle - \langle \dot{W}_f \rangle + \langle \dot{Q}_1 \rangle + \langle \dot{Q}_2 \rangle = 0. \quad (17)$$

These equations allow us to define the conditions for which the demon can reverse the flow without any energy exchange with the system.

In the absence of the demon the heat flux is given by Eqs. (6), i.e., $\langle \dot{Q}_2 \rangle = -\langle \dot{Q}_1 \rangle < 0$. Using the demon we want to reverse this flow, making $\langle \dot{Q}_2 \rangle \gg 0$ but keeping $\langle \dot{Q}_1 \rangle = -\langle \dot{Q}_2 \rangle$ because an observer, who measures the heat flux of the system, has to establish that heat flows from the cold to the hot reservoir. The condition $\langle \dot{Q}_1 \rangle = -\langle \dot{Q}_2 \rangle$ has two main consequences. First, it reduces Eq. (17) to

$$\langle \dot{Q}_d \rangle - \langle \dot{W}_f \rangle = 0, \quad (18)$$

which indicates that all the power supplied by V_f is dissipated in the demon reservoirs and not in the system reservoirs.

Second, applying it to Eqs. (13) and (14) we find that

$$\frac{V_t^2}{R_2} = A \frac{R_t}{R_d} (T_1 - T_d) + B(T_2 - T_d). \quad (19)$$

Finally, using Eq. (19) and the condition $\langle \dot{Q}_2 \rangle \gg 0$ in Eq. (14), we compute the range of T_d , where the spontaneous process is reversed, finding

$$T_d \leq T_1 - \frac{R_d}{R_2} (T_2 - T_1). \quad (20)$$

Equations (19) and (20) fix the conditions that allow the demon to reverse the system mean heat flux without mean energy exchanges [Eq. (18)] between the demon and the system. Equation (19) indicates that the fraction of the power injected by the demon and dissipated in R_2 [V_t^2/R_2 in Eq. (14)] is compensated by the heat extracted from the system baths (see also Sec. VI in Ref. [24]). We can also prove that owing to Eq. (19) the demon does not perform any work on the system. Indeed, the total work performed by the demon on the system is $\langle \dot{W}_{d,s} \rangle = \langle \dot{W}_{d,1} \rangle + \langle \dot{W}_{d,2} \rangle$, where $\langle \dot{W}_{d,1} \rangle$ and $\langle \dot{W}_{d,2} \rangle$ are the works performed on subsystems 1 and 2, respectively. These can be computed using Eqs. (7) and (8) in which we see that a ‘‘force’’ proportional to $q_{d1} + q_{d2}$ is applied on the two subsystems. Thus the work per unit time of these forces is [20]

$$\langle \dot{W}_{d,1} \rangle = \frac{C}{X_t} \langle \dot{q}_1 (q_{d1} + q_{d2}) \rangle, \quad (21)$$

$$\langle \dot{W}_{d,2} \rangle = -\frac{C_1 + C}{X_t} \langle \dot{q}_2 (q_{d1} + q_{d2}) \rangle. \quad (22)$$

From these two works [24] we obtain for the total work

$$\langle \dot{W}_{d,s} \rangle = -A \frac{R_t}{R_d} (T_1 - T_d) - B(T_2 - T_d) + \frac{V_t^2}{R_2}. \quad (23)$$

We clearly see that if the condition on V_t [Eq. (19)] is verified, then $\langle \dot{W}_{d,s} \rangle = 0$, i.e., no work is done by the demon on the system. Thus Eqs. (19) and (18) ensure that the total energy flux from the demon to the system is zero.

However, the demon produces entropy and the total entropy production rate $\langle \dot{S} \rangle$ is positive in spite of the fact that the system entropy production rate $\langle \dot{S}_s \rangle = \langle \dot{Q}_2 \rangle (1/T_2 - 1/T_1)$ is negative, because $\langle \dot{Q}_2 \rangle \gg 0$ and $T_2 > T_1$ when the demon is ‘‘on.’’ The total entropy production rate is

$$\langle \dot{S} \rangle = \frac{\langle \dot{Q}_d \rangle}{T_d} + \langle \dot{Q}_2 \rangle \left(\frac{1}{T_2} - \frac{1}{T_1} \right). \quad (24)$$

To show that $\langle \dot{S} \rangle \gg 0$, we start by taking into account that $\langle \dot{Q}_d \rangle = \langle \dot{W}_f \rangle$ [see Eq. (18)] and that $\langle \dot{W}_f \rangle \gg \frac{V_t^2}{R_2}$ because we have seen that $\frac{V_t^2}{R_2}$ is a fraction of the total power injected into the system by the demon source [24].

Furthermore, as we want $\langle \dot{Q}_2 \rangle \gg 0$, then from Eq. (14) we have that $V_t^2/R_2 > \langle \dot{Q}_2 \rangle$ as the other terms are negative because $T_2 > T_1 > T_d$. As a consequence, $\langle \dot{Q}_d \rangle / T_d > \langle \dot{Q}_d \rangle (1/T_1 - 1/T_2) > \langle \dot{Q}_2 \rangle (1/T_1 - 1/T_2)$ and we find $\langle \dot{S} \rangle \gg 0$.

These results on the effect of the demon on the system can be checked by comparing the heat fluxes computed from Eqs. (13) and (14) with those obtained by the direct numerical integration of Eqs. (7)–(10), where the four $\langle \dot{Q}_k \rangle = \langle v_k \dot{q}_k \rangle$ are directly computed using Stratonovich integrals.

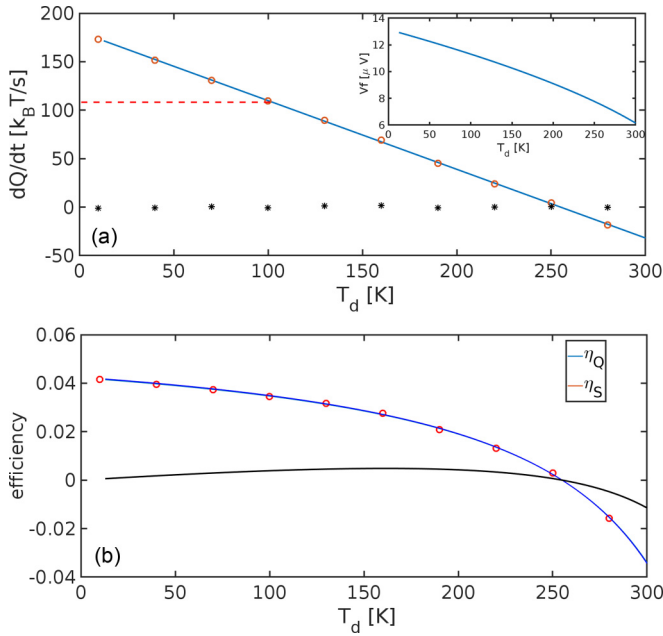


FIG. 2. (a) Heat fluxes as a function of the demon temperature T_d : $\langle \dot{Q}_2 \rangle$ (blue line) computed when the demon is on, using Eqs. (13)–(16) and the condition for V_i^2 [Eq. (19)]; $\langle \dot{Q}_1 \rangle$ (horizontal red dashed line) computed [Eq. (6)] when the demon is “off”; $\langle \dot{Q}_2 \rangle$ (red circles) and $\langle \dot{Q}_2 \rangle + \langle \dot{Q}_1 \rangle$ (black stars) obtained from the direct numerical simulation of Eqs. (7)–(10). (b) Demon efficiencies as a function of T_d : η_s (black line) and η_Q (blue line, red circles) computed from Eqs. (14), (16), and (25) (continuous lines) and obtained from the direct numerical simulations of Eqs. (7)–(10) (red circles). The parameters used to compute the curves in (a) and (b) are $T_1 = 300$ K, $T_2 = 450$ K, $C = 1$ nF, $C_1 = C_2 = 100$ pF, $R_1 = R_2 = 10$ M Ω , $R_d = 3$ M Ω , and $C_d = 50$ pF.

This comparison is done using for the system components (i.e., R_1, R_2, C_1, C_2, C) the values of the experiment of Refs. [19,20]. For the demon, we chose for C_d a typical wiring value and we fixed $R_d < R_2$ for having a reasonable range of T_d [see Eq. (20)]. All the components and temperatures values are indicated in the caption of Fig. 2. In Fig. 2(a) the horizontal red dashed line indicates $|\langle \dot{Q}_2 \rangle|$ at $T_2 - T_1 = 150$ K computed from Eq. (6) when the demon is “off.” When the demon is “on” the value of \dot{Q}_2 computed from Eqs. (14) and that obtained from direct numerical simulation agree. Most importantly, for $T_d < 250$ K the heat flows from the cold to the hot thermal bath. The values of V_i necessary for implementing the demon conditions [Eq. (19)] are plotted in the inset, and

indeed for these values of V_i we see that $\langle \dot{Q}_2 \rangle + \langle \dot{Q}_1 \rangle = 0$ in the numerical simulation. It is important to notice that the necessary V_i is of the order of a few microvolts, meaning that it can be easily obtained by two thermocouples coupled with a cold and an hot bath, for example, T_1 and T_2 .

The demon efficiency can be defined in two ways. As the demon does not exchange any work and heat with the system, then the efficiency can be defined in terms of entropy production rates, which has been used in other contexts [25–27]. Another way to define efficiency is in terms of the energy fluxes. Specifically, these efficiencies are

$$\eta_s = -\frac{\dot{S}_s}{\dot{S}_d} \quad \text{and} \quad \eta_Q = \frac{\langle \dot{Q}_2 \rangle}{\langle \dot{W}_f \rangle}. \quad (25)$$

We see that η_s is the ratio between the entropy of the nonspontaneous process divided by the entropy of the spontaneous process whereas η_Q is the ratio between the reversed heat flux in the system divided by the work performed by the demon to achieve the goal. These two quantities are plotted in Fig. 2(b) as a function of T_d , and we observe that $\eta_s < 1\%$ and $\eta_Q < 4\%$, i.e., in order to achieve its goal the demon has to do a lot of work with a very large entropy production rate.

To conclude, let us first point out that we do not discuss here whether the OEMD [15] acts as a real demon or it is only an “entropic refrigerator” [28]. We leave this question to future works, because the main purpose of this Rapid Communication is to demonstrate that the original idea of the OEMD [15] can be simplified and applied to electric circuits. We use a simple one as a proof of principle but other complex circuits can be implemented. We proved that the OEMD reverses the spontaneous heat processes with no mean energy flux between the system and demon, which has a single bath and a DC forcing (powered by thermocouples) instead of two baths with colored noise as in Refs. [15,16]. The demon has a small efficiency and a very large positive entropy production that compensates the negative one of the system. Our results are very general because they are based on four coupled Langevin equations, which model not only electric circuits, but many mesoscopic systems, which are in principle controllable by OEMDs.

We acknowledge useful discussions with R. S. Whitney. This work has been supported by the FQXi Foundation, Grant No. FQXi-IAF19-05, “Information as a fuel in colloids and superconducting quantum circuits.”

[1] E. Lutz and S. Ciliberto, *Phys. Today* **68** (9), 30 (2015).
 [2] J. M. R. Parrondo, J. M. Horowitz, and T. Sagawa, *Nat. Phys.* **11**, 131 (2015).
 [3] S. Toyabe, T. Sagawa, M. Ueda, M. Muneyuki, and M. Sano, *Nat. Phys.* **6**, 988 (2010).
 [4] C. Elouard, D. Herrera-Martí, B. Huard, and A. Auffèves, *Phys. Rev. Lett.* **118**, 260603 (2017).
 [5] T. Admon, S. Rahav, and Y. Roichman, *Phys. Rev. Lett.* **121**, 180601 (2018).

[6] Y. Masuyama, K. Funo, Y. Murashita, A. Noguchi, S. Kono, Y. Tabuchi, R. Yamazaki, M. Ueda, and Y. Nakamura, *Nat. Commun.* **9**, 1291 (2018).
 [7] G. N. Price, S. T. Bannerman, K. Viering, E. Narevicius, and M. G. Raizen, *Phys. Rev. Lett.* **100**, 093004 (2008).
 [8] J. V. Koski, V. F. Maisi, J. P. Pekola, and D. V. Averin, *Proc. Natl. Acad. Sci. USA* **111**, 13786 (2014).
 [9] J. V. Koski, A. Kutvonen, I. M. Khaymovich, T. Ala-Nissila, and J. P. Pekola, *Phys. Rev. Lett.* **115**, 260602 (2015).

- [10] A. C. Barato and U. Seifert, *Europhys. Lett.* **101**, 60001 (2013).
- [11] N. Shiraishi, S. Ito, K. Kawaguchi, and T. Sagawa, *New J. Phys.* **17**, 045012 (2015).
- [12] A. B. Boyd, D. Mandal, and J. P. Crutchfield, *New J. Phys.* **18**, 023049 (2016).
- [13] M. L. Rosinberg and J. M. Horowitz, *Europhys. Lett.* **116**, 10007 (2016).
- [14] Z. Lu and C. A. Jarzynski, *Entropy* **21**, 65 (2019).
- [15] R. Sanchez, J. Splettstoesser, and R. S. Whitney, *Phys. Rev. Lett.* **123**, 216801 (2019).
- [16] F. Hajiloo, R. Sánchez, R. S. Whitney, and J. Splettstoesser, *Phys. Rev. B* **102**, 155405 (2020).
- [17] N. Freitas, J.-C. Delvenne, and M. Esposito, *Phys. Rev. X* **10**, 031005 (2020).
- [18] R. van Zon, S. Ciliberto, and E. G. D. Cohen, *Phys. Rev. Lett.* **92**, 130601 (2004).
- [19] S. Ciliberto, A. Imparato, A. Naert, and M. Tanase, *Phys. Rev. Lett.* **110**, 180601 (2013).
- [20] S. Ciliberto, A. Imparato, A. Naert, and M. Tanase, *J. Stat. Mech.* (2013) P12014.
- [21] R. Filliger and P. Reimann, *Phys. Rev. Lett.* **99**, 230602 (2007).
- [22] S. Cerasoli, V. Dotsenko, G. Oshanin, and L. Rondoni, *Phys. Rev. E* **98**, 042149 (2018).
- [23] N. Garnier and S. Ciliberto, *Phys. Rev. E* **71**, 060101(R) (2005).
- [24] See Supplemental Material at <http://link.aps.org/supplemental/10.1103/PhysRevE.102.050103> for further details on the demon and on the calculation of the currents, the works, and dissipated energies.
- [25] G. Verley, T. Willaert, C. Van den Broeck, and M. Esposito, *Phys. Rev. E* **90**, 052145 (2014).
- [26] M. Poletti, G. Verley, and M. Esposito, *Phys. Rev. Lett.* **114**, 050601 (2015).
- [27] J.-F. Derivaux and Y. De Decker, *J. Stat. Mech.* (2019) 034002.
- [28] N. Freitas and M. Esposito, [arXiv:2011.04497](https://arxiv.org/abs/2011.04497).